Preprint Title Effect of pulsed electrospinning process variables on the size of polymer fibers established with a 2^3 factorial design

Authors Aleksandra Bartkowiak, Marcin Grzeczkowicz and Dorota Lewińska

Publication Date 19 Feb. 2024

Article Type Full Research Paper

ORCID® iDs Aleksandra Bartkowiak - https://orcid.org/0000-0002-6213-4798;
Dorota Lewińska - https://orcid.org/0000-0002-9978-9157

Effect of pulsed electrospinning process variables on the size of polymer fibers established with a 2^3 factorial design

Aleksandra Bartkowiak*[1], M. Grzeczkowicz[1], Dorota Lewińska[1]

[1] *Nalecz Institute of Biocybernetics and Biomedical Engineering Polish Academy of Sciences, Ks. Trojdena 4, 02-109 Warsaw, Poland*

abartkowiak@ibib.waw.pl

*Corresponding author

Abstract

In the present study, the influence of electrical parameters of the pulsed electrospinning process, such as electrical voltage, frequency of the pulses and pulse duration on the structure of the nonwovens obtained was determined for the first time. It was found that all the parameters studied strongly influence the average diameter of the fibres obtained, and that the pulsed electrospinning process carried out under specific conditions makes it possible to obtain, among other things, bimodal nonwovens. In addition, a 2^3 factorial design was used to determine how the selected electrical parameters of the pulsed electrospinning process affect the structure of the resulting electrospun mats. It was shown, among other things, that by appropriately selecting the parameters of the electrospinning process, the thickness of the fibres can be controlled, resulting in nonwovens with the desired morphology.

Keywords: bimodal structure; electrospinning; factorial design; polymer fiber; pulsed voltage

1. INTRODUCTION

Electrospinning is a simple and effective technique that allows the production of polymer fibres. Over the past few decades, a staggering number of fibrous materials have been developed for applications including filtration, enzyme immobilisation, controlled drug release systems,

tissue engineering and the manufacture of dressings [1,2]. An extremely large number of polymers, both natural (chitosan, collagen, gelatine) and synthetic (polyvinylpyrrolidone, poly(lactic acid), polyacrylonitrile, poly(ethylene oxide), poly(acrylic acid), polyacrylamide and poly(vinyl alcohol)), are used to produce fibres [3,4].

In the electrospinning process, the polymer is pumped into a spinning nozzle to which a strong electric field is applied. This results in the distribution of electrical charges on the surface of the polymer jet leaving the spinning nozzle. One electrode, with a positive potential, is connected to the nozzle with the polymer solution, the other, with a negative potential, to a grounded collector. When the electrical voltage increases, the semicircular surface of the polymer at the exit of the nozzle elongates to form a characteristic conical shape called a Taylor cone. A further increase in electrical voltage, up to a critical value, causes the Coulombic forces, responsible for the repulsion of opposing charges, to overcome the surface tension forces of the polimer jet. The discharged polymer solution beam is ejected from the nozzle tip towards the collector. Meanwhile, the solvent is evaporated and fibres are collected on the grounded collector [5–7].

The parameters affecting the formation of fibres during the electrospinning process and their morphology can be divided into two main groups: (1) the physicochemical properties of the polymer solution, such as viscosity, conductivity, surface tension, which depend on the molecular weight of the polymer, the type of solvent and the concentration of the polymer solution; (2) the parameters of the electrospinning process, such as the electrical voltage, the flow rate of the polymer solution, the distance between the spinning nozzle and the collector and the environmental parameters (temperature, humidity, airflow in the chamber) [1,5,8]. Understanding how each parameter affects the product obtained by electrospinning is crucial to achieving the desired result.

As is well known, the electrical voltage influences the electrical force that stretches the polymer jet into the finest fibre and thus affects the diameter of the fibers and morphology of the nonwovens. It is widely accepted that electrical voltage is one of the most important parameters determining the morphology and diameter of the fibres obtained by electrospinning process. Direct-current voltage (DCV) is commonly used in the electrospinning process [9–11], while pulsed voltage (PV) is used much less frequently [12–15]. In the second process variant, an electrical voltage is applied to the nozzle in the form of pulses of a preset frequency and pulse duration. The use of pulsed voltage (PV) in the electrospinning process therefore provides an additional opportunity to control parameters such as the frequency of the pulses and the pulse duration, which can significantly affect the morphologies of the nonwovens obtained.

In one of the first papers on the use of pulsed voltage (PV) in the electrospinning process, Li et al. [12] reported the effects of electrical voltage, polyvinylpyrrolidone (PVP) solution flow rate, frequency and pulsed electric field duty cycle on the average diameter and diameter distribution of electrospun fibres. Among other things, it was found that the effect of frequency on fibre diameter was not significant. Furthermore, the use of PV allowed thinner fibres to be obtained. In turn, Mirek et al. in their work [15] demonstrated that the type of electric voltage applied in the process influences the structure of the electrospun mats produced. The electrospinning process of polyvinylpyrrolidone (PVP) and polylactide (PLA) solutions was carried out using direct-current voltage (DCV) and pulsed voltage (PV) of selected frequencies (20, 50 and 100 Hz) and a pulse duration of 5 ms. The parameter that had the strongest effect on the structure of the fibre mats was frequency of the pulses. In addition, the authors found that the use of pulsed voltage (PV) provided, among other things, better stability in the electrospinning process and allowed a greater variety in the structures of electrospun mats.

For a very long time it was thought that the ideal nonwoven fabric consisted of smooth and homogeneous fibers with a relatively narrow distribution of average fiber diameters. In recent

years, it has been proven that the production of nonwoven fabrics with bimodal and multimodal structures, as well as those containing spheroidal elements in the structure (e.g., bead-on-string nonwoven fabrics) open up new possibilities for biomedical engineering applications, among others [16–22]. Hence, it seems necessary to determine how changing the electrical parameters of the pulsed electrospinning process will affect the morphology of the resulting nonwovens.

Earlier work found, among other things, that: the diameter of the fibre without beads depends mainly on the electrical voltage, while the electrical voltage was a factor with a secondary effect on fibre and bead size [23]; the morphological and mechanical properties of the obtained nonwovens show a clear correlation with the applied voltage [24]; the morphology of the nonwovens produced is influenced by both the waveform (square, sine, triangle) and the frequency of the alternating current (AC) high-voltage signal applied [25]. As a result, nonwovens containing smooth fibres and those having beads, spindles and/or helical fibres in their structure were obtained [25]. Moreover, it has been proven that higher frequencies favour the formation of thicker fibres [25].

The aim of this study was to determine the influence of all electrical parameters, such as electrical voltage (U), frequency of the pulses (f) and pulse duration (τ), on the pulsed electrospinning process and the structure of the nonwovens obtained. A polyvinylpyrrolidone (PVP) solution was electrospinning using a pulse voltage (PV) with a set frequency in the range 10-100 Hz and a pulse duration in the range 1-9 ms. In addition, a factorial design was used to determine how the selected electrical parameters of the electrospinning process affect the structure of the resulting electrospun mats. Factorial design is widely used to study the effects of experimental factors and the interactions between these factors, that is, how the effect of one factor changes with the level of the other factors in the response. The advantages of factorial design are the relatively low cost, the much smaller number of experiments and the increased ability to assess interactions between variables [26,27].

Only a few papers used factor analysis to evaluate the properties of the solution used for electrospinning and the effect of the process parameters on the morphology of the nonwovens produced [23, 28–31] However, the authors' conclusions are clear: factor analysis is a useful tool for designing fibre mats with the desired structure and properties to meet the requirements of various applications, i.e. drug delivery, dressings or tissue engineering. The 2^3 full factorial design has previously been successfully applied by Korycka et al. [23], among others, to determine the relationship between factors, i.e. polyvinylpyrrolidone (PVP) solution flow rate, solution viscosity and electrical voltage, and the diameter of homogeneous and bead-on-string fibres produced by the electrospinning process. In our work, we will determine for the first time the relationship between electrical parameters and the morphology of electrospun mats from an alcoholic polyvinylpyrrolidone (PVP) solution.

2. EXPERIMENTAL

Materials

Polyvinylpyrrolidone (PVP, M_w=1300 kDa) was purchased from Sigma-Aldrich. PVP solution (17% concentration) was prepared by dissolving the polymer in 96% (w/w) ethanol purchased from Polmos. The solution viscosity at 25 °C was 1.047 Pa·s.

Electrospinning setup

The electrospinning process was carried out using the setup shown in Figure 1. The system consisted of: a high-voltage pulse generator, an infusion pump connected by a drain to a steel nozzle (inner/outer diameter = 0.63/0.9 mm) and a grounded circular aluminum collector (thickness = 0.12 mm, diameter = 100 mm) placed at a distance of 15 cm from the nozzle tip. The polymer solution was delivered to the nozzle at a flow rate of 0.9 ml/h. The electrospinning proces was carried out using varying values of electric voltage (*U*), frequency of the pulses (*f*)

and pulse duration (τ). Electrical voltages of 8 kV and 15 kV were used. Electrical pulses were delivered with a frequency in the range of 10-100 Hz (changing in 10 Hz increments) and a duration in the range of 1-9 ms (changing in 1 ms increments). The resulting product was deposited on the collector for 3 min. All experiments were conducted at 25 °C. The ambient humidity did not exceed 40%.

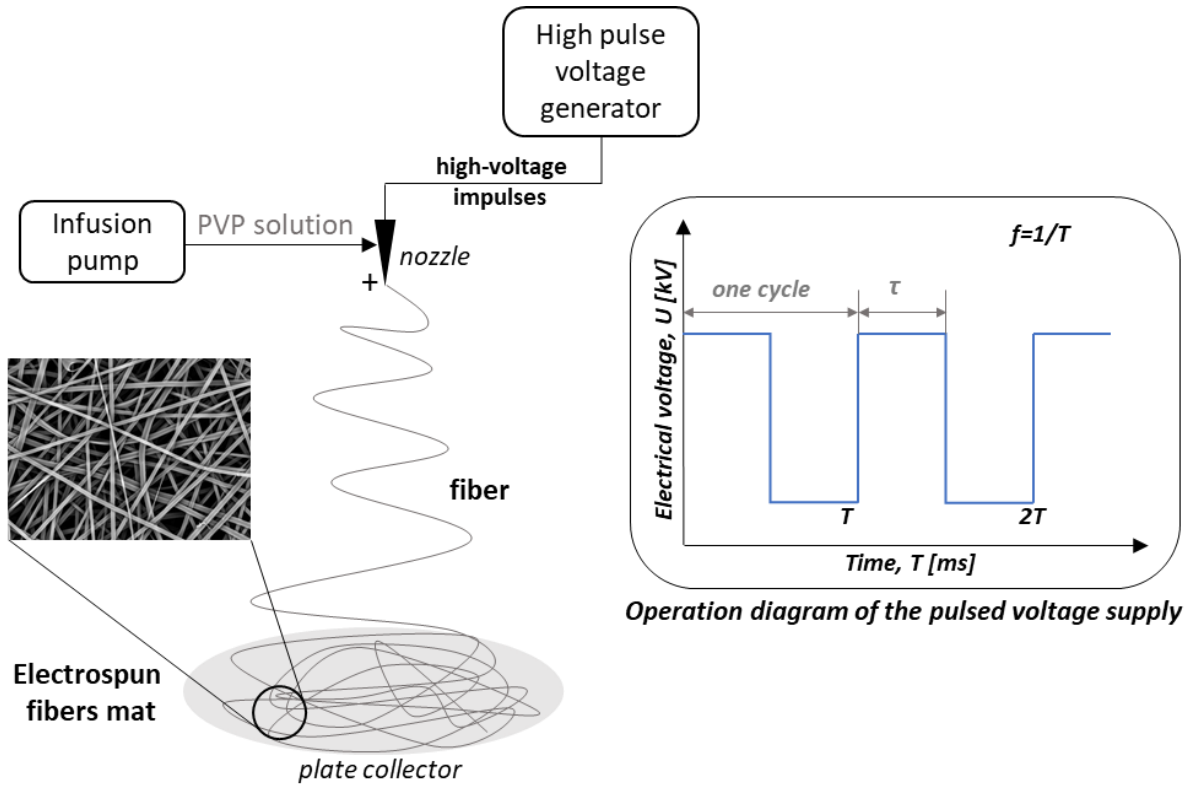

Figure 1: Scheme of the electrospinning process setup with an operation diagram of the pulsed voltage (PV) supply (blue line).

Morphology of electrospun mats

The morphology of the obtained polymer electrospun mats was characterized by two parameters: the size of the average fiber diameter *D* and the uniformity of the fibers in terms of their diameter. Both parameters were determined based on scanning electron microscopy (SEM, Hitachi TM-1000) images. Before SEM images were taken, a thin layer of gold (about 10 nm) was sputtered onto each sample of the electrospun mats. Using the computer software provided

with the microscope, the diameters of 50 randomly selected fibers obtained by electrospinning the PVP solution under different electrical conditions of the process were measured. From the values obtained, the average diameters for each fiber (*D*), standard deviation (±SD) and coefficient of variation (CV) were calculated. CV was calculated based on the formula: $CV = \frac{SD}{D} \cdot 100\%$.

Factorial design

The direct influence of process factors and the possible effects of their interaction can be predicted using the factor design method. The effects of selected electrical parameters of the electrospinning process (such as electrical voltage (*U*), frequency of the pulses (*f*) and pulse duration (τ)) on the formation and morphology of the produced fibers were investigated using a factorial design.

In this method, in order to set up a two-level factor plan, it is necessary to define the experimental domain. Each factor is assigned a high (+) and low (-) level. The complete model system includes all combinations of extreme settings of experimental factors. A model with *k* factors consists of 2^k experimental runs. For the case with three experimental factors, the response surface model is as follows:

$$y = a_0 + \sum_{i=1}^{3} a_i x_i + \sum_{i=1}^{3}\sum_{j=1}^{3} a_{ij} x_i x_j + a_{123} x_1 x_2 x_3 \qquad (1)$$

where: y – the response; a_0, a_i, a_{ij}, and a_{123} – the coefficients; x_1, x_2, x_3, x_i, and x_j - the experimental factors. The constant term a_0 corresponds to the response value when all parameters are at the center point at an average level ($x_1 = x_2 = x_3 = 0$).

The coefficients (a) are determined by the coded values of the factors (high factor level is +1 and low factor level is –1). For three factors, the experimental system takes the form of a matrix:

$$\begin{array}{c} Experiment \\ 1 \\ 2 \\ 3 \\ 4 \\ 5 \\ 6 \\ 7 \\ 8 \end{array} \begin{bmatrix} x_1 & x_2 & x_3 \\ -1 & -1 & -1 \\ -1 & -1 & +1 \\ -1 & +1 & -1 \\ -1 & +1 & +1 \\ +1 & -1 & -1 \\ +1 & -1 & +1 \\ +1 & +1 & -1 \\ +1 & +1 & +1 \end{bmatrix} \quad (2)$$

To calculate the a_i–a_{ijk} coefficients, the **X** matrix is expanded with column *I* for the constant expression, and columns for all possible factor interactions in the model as:

$$\begin{array}{c} Experiment \\ 1 \\ 2 \\ 3 \\ 4 \\ 5 \\ 6 \\ 7 \\ 8 \end{array} \begin{bmatrix} I & x_1 & x_2 & x_3 & x_1 \cdot x_2 & x_1 \cdot x_3 & x_2 \cdot x_3 & x_1 \cdot x_2 \cdot x_3 \\ +1 & -1 & -1 & -1 & +1 & +1 & +1 & -1 \\ +1 & -1 & -1 & +1 & +1 & -1 & -1 & +1 \\ +1 & -1 & +1 & -1 & -1 & +1 & -1 & +1 \\ +1 & -1 & +1 & +1 & -1 & -1 & +1 & -1 \\ +1 & +1 & -1 & -1 & -1 & -1 & +1 & +1 \\ +1 & +1 & -1 & +1 & -1 & +1 & -1 & -1 \\ +1 & +1 & +1 & -1 & +1 & -1 & -1 & -1 \\ +1 & +1 & +1 & +1 & +1 & +1 & +1 & +1 \end{bmatrix} \quad (3)$$

Consequently, the experimental series can be summarized by means of the matrix relation:

$$\boldsymbol{y} = \boldsymbol{X} \cdot \boldsymbol{A} \quad (4)$$

which in the described case corresponds to:

$$\begin{bmatrix} y_1 \\ y_2 \\ y_3 \\ y_4 \\ y_5 \\ y_6 \\ y_7 \\ y_8 \end{bmatrix} = \begin{bmatrix} +1 & -1 & -1 & -1 & +1 & +1 & +1 & -1 \\ +1 & -1 & -1 & +1 & +1 & -1 & -1 & +1 \\ +1 & -1 & +1 & -1 & -1 & +1 & -1 & +1 \\ +1 & -1 & +1 & +1 & -1 & -1 & +1 & -1 \\ +1 & +1 & -1 & -1 & -1 & -1 & +1 & +1 \\ +1 & +1 & -1 & +1 & -1 & +1 & -1 & -1 \\ +1 & +1 & +1 & -1 & +1 & -1 & -1 & -1 \\ +1 & +1 & +1 & +1 & +1 & +1 & +1 & +1 \end{bmatrix} \cdot \begin{bmatrix} a_0 \\ a_1 \\ a_2 \\ a_3 \\ a_{12} \\ a_{13} \\ a_{23} \\ a_{123} \end{bmatrix} \quad (5)$$

And finally, the coefficients are determined by solving Eq. 6 using the least squares method:

$$\boldsymbol{A} = (\boldsymbol{X^T} \cdot \boldsymbol{X})^{-1} \cdot \boldsymbol{X^T} \cdot \boldsymbol{y} \quad (6)$$

where: $\boldsymbol{A}$ – set of the coefficients, $\boldsymbol{X^T}$ – transposed matrix and **y** – response.

The absolute value of a given coefficient a determines the influence of the analyzed model factor on the response. It is assumed that the higher the value of the coefficient, the stronger the

relationship between the given factor and the response. In turn, the nature of this relationship is indicated by the sign of the coefficient: a positive coefficient means that the value of the response increases as the value of the factor increases, while a negative coefficient means that the relationship is inversely proportional.

Selection of proces factors for the factorial design

Conducting a 2^3 full factorial analysis requires the selection of experimental variants for the electrospinning process carried out under extreme conditions. The process parameters are shown in Table 1. The high (maximum) and low (minimum) levels of process factors (U, f, τ) were assigned values of +1 and -1, respectively. f=30 Hz was chosen as the low frequency level, as below this frequency value fibre electrodeposition does not occur.

Table 1: Process variables selected for the 2^3 factorial analysis for fiber diameter in fibrous mats

Parameter	Low level (-1)	High level (+1)
U – electrical voltage	8 kV	15 kV
f – frequency of the pulses	30 Hz	100 Hz
τ – pulse duration	1 ms	9 ms

3. RESULTS AND DISCUSSION

Effect of electrical parameters on the diameters of the obtained fibers

A series of experiments were conducted to establish the relationship between the electrical parameters of the electrospinning proces (U, f ,τ) and the diameter of the fibres (D) obtained. The process was carried out using high voltages of 8 kV and 15 kV. Figures 2 and 3 show the dependence of average fibre diameters on frequency of the pulses (30-100 Hz) (A) and dependence of average fibre diameters on pulse duration (1-10 ms) (B).

Analysis of Figure 2A makes it possible to divide the curves showing the dependence of the average diameters of the fibres obtained on the frequency (*f*) into two main groups. The first group includes the curves when τ=1-2 ms and 5-10 ms for which the fibre thickness varies slightly (by 15-20%) depending on the set frequency. When τ=1-2 ms is used, the values of the average diameters of the fibres obtained range from about 1 to 1.6 µm for *f* in the range 30-90 Hz. Only at *f*=100 Hz is a drastic change observed in the diameter of the fibres obtained (*D* is then about 3 µm). On the other hand, when τ=5-10 ms is used, the values of the average diameters of the fibres obtained range from approx. 2.5 to 3 µm for f over the entire range investigated. It should be noted that a clearly distinct group are the curves when τ=3-4 ms, as the values of the average diameters of the fibres obtained fall within a wide range (from approx. 1 to more than 3 µm).

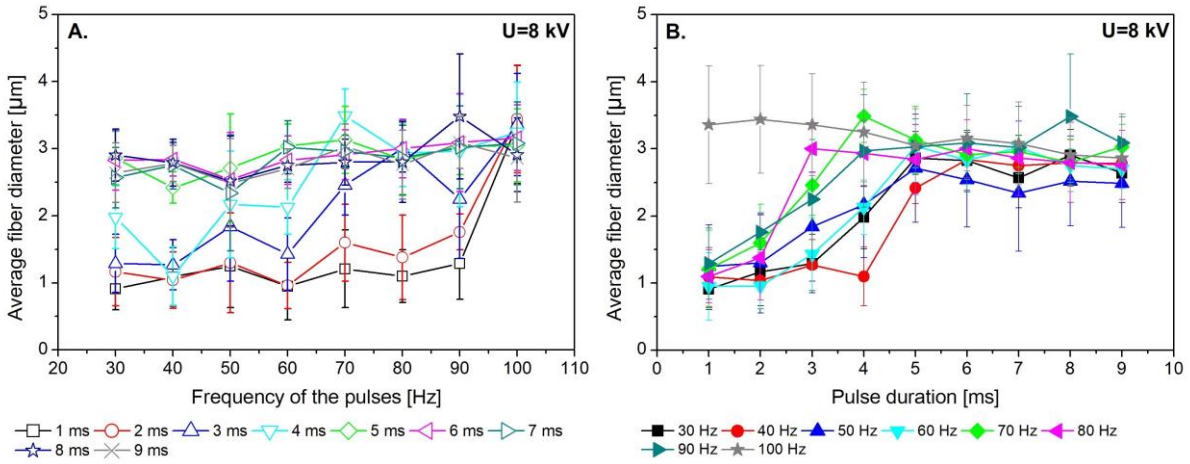

Figure 2: Dependence of average fibre diameters (*D*) on: (A) frequency of the pulses (30-100 Hz) and (B) pulse duration (1-10 ms) for a process conducted at *U*=8 kV.

Overall, the analysis of Figure 2B confirms that the mean fibre diameters change over a wide range of set frequency of the pulses (30-100 Hz) and pulse duration (1-9 ms). For *f*=30-90 Hz, a step increase in mean fibre diameters is observed, and the critical pulse duration τ at which a drastic change in fibre diameters occurs is 4-5 ms. This increase is almost threefold in most cases, and the value of *D* varies over a wide range from about 1 to about 3 µm. The

situation is completely different when the process is run at *f*=100 Hz: then the average diameter of the fibres formed is about 3 µm regardless of the set τ. These results prove that an appropriate choice of *f* and τ while applying an electric voltage of 8 kV results in fibres with the desired diameter. From the analysis of the morphology of the nonwovens obtained by electrospinning at an electrical voltage of 8 kV, it can be concluded that working in lower frequency ranges and at lower pulse durations allows nonwovens of very different thicknesses to be obtained. According to available literature data, the diameters of microspheres obtained by electrospraying a polymer solution using pulsed voltage (PV) strongly depend on the set frequency and pulse duration. However, they show the opposite effect to that observed in this study with the application of an electrical voltage of the order of 8 kV. The authors of previous work observed a decrease in *D* with increasing f and τ [32,33]. These differences between previous studies and those described in this paper are probably due to the different physico-chemical properties of the polymer solutions used for electrospinning/electrospraying.

The situation is different when the system is operated at higher electrical voltages (Figure 3). Under conditions of *U*=15 kV, the average diameters of the fibres formed during the electrospinning process are also in the range of approximately 1 to 3 µm but decrease with increasing frequency in the system (Figure 3A) (the exception being fibres obtained at τ=1 ms – black curve).

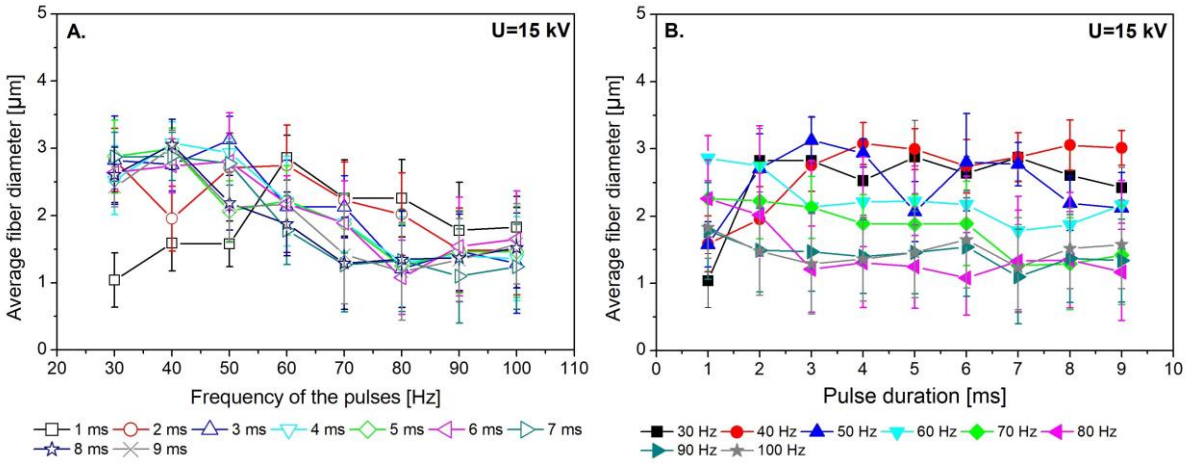

Figure 3: Dependence of average fibre diameters (*D*) on: (A) frequency of the pulses (30-100 Hz) and (B) pulse duration (1-10 ms) for a process conducted at *U*=15 kV.

As mentioned above, similar effects are observed in the classic electrospray method [32,33]. In addition, in a study by Mirek et al. [15], the application of an electrical voltage of *U*=15 kV and a frequency of the pulses of *f*=100 Hz also led to the electrospinning of an 8% PVP solution to produce fibres with diameters more than twice as small as when electrospinning at *f*=20 Hz. An analysis of Figure 3A shows that the greatest changes in *D* values are observed when *f*=30-50 Hz is applied. In other cases, the changes in average fibre diameters shown in the curves are of the order of approximately 20-40% (Figure 4B) and somewhat resemble the curve obtained when *U*=8 kV and *f*=100 Hz (Figure 3B; gray star marker), indicating that at high frequencies, even a large increase in the charge delivered to the system does not cause a drastic change in *D* values. It should also be noted that the decrease in mean fibre diameter at very high frequencies and high pulse durations confirms the parallel formation of a finer fibre fraction and the formation of fibres characterised by a bimodal fibre distribution (Figure 5C).

Conventional single-needle electrospinning usually obtains nonwovens with monomodal fibre distributions (one fibre population of very similar thickness in the structure) covering both the nano- and micro-scale. However, there are several literature reports [16,17,19–22] on obtaining nonwovens with bi- and multimodal fibre distributions obtained by both single-needle and multi-needle electrospinning. Such nonwovens are characterised by the presence of two or more fibre populations of very different thickness in the structure. In recent years, nonwovens with bi- and multimodal structures have been proven to have broad application prospects in biomedicine and other fields [16,17].

As mentioned earlier, fibre formation by electrospinning was only possible with a charge at pulse frequencies in the range 30-100 Hz. The lack of fibre formation from the PVP solution at pulse frequencies in the range 10-20 Hz was probably due to insufficient charge delivered to

the capillary nozzle. Depending on the electrical parameters (U, f, τ) of the process, nonwoven fabrics with different morphologies were obtained.

Figures 4 and 5 show SEM images of selected electrospun fibre mats obtained under specific process conditions, histograms and estimated coefficients of variation (CV %) values. SEM images and fibre diameter distribution histograms were taken for nonwovens obtained during the electrospinning process carried out at electrical voltages of 8 kV or 15 kV, pulse frequencies in the range of 30-100 Hz and pulse durations in the range of 1-10 ms. The examples presented (Figures 4-5) show nonwovens with different fibre diameter distribution. Taking into account the histograms, three basic types of nonwovens were distinguished: monomodal (Figure 4 and 5A), characterized by a low CV value and a single pick in the histogram, quasi-bimodal (Figure 5B), characterised by CV value between 30 and 50% and two combined peaks per histogram CV and bimodal (Figure 5C) with a high CV value and two well-separated peaks in the histogram.

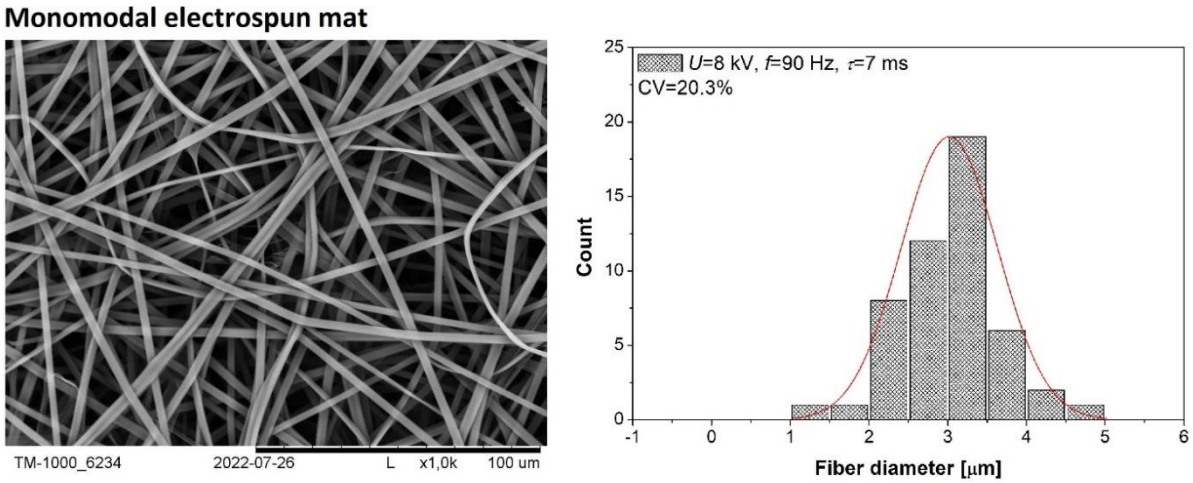

Figure 4: Morphology and distribution of fibre diameters in electrospun mats produced at electrical voltage (U)=8 kV, frequency of the pulses (f)=90 Hz and pulse duration (τ)=7 ms. Normal distribution (solid line on the graph).

(A) Monomodal electrospun mat

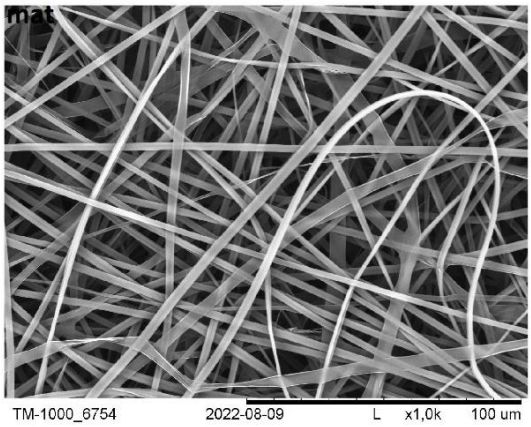

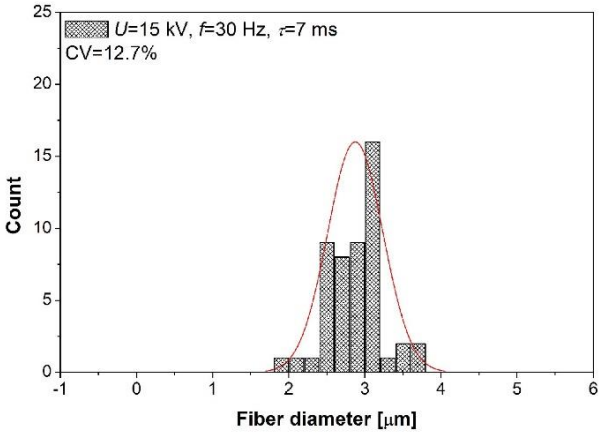

(B) Quasi-bimodal electrospun mat

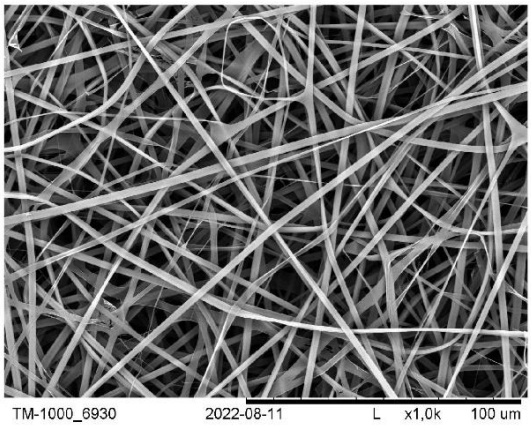

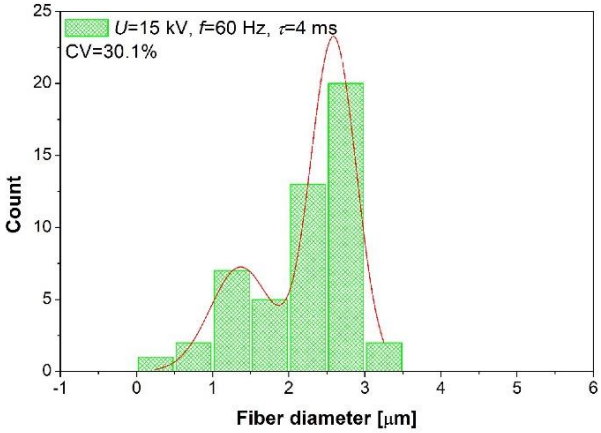

(C) Bimodal electrospun mat

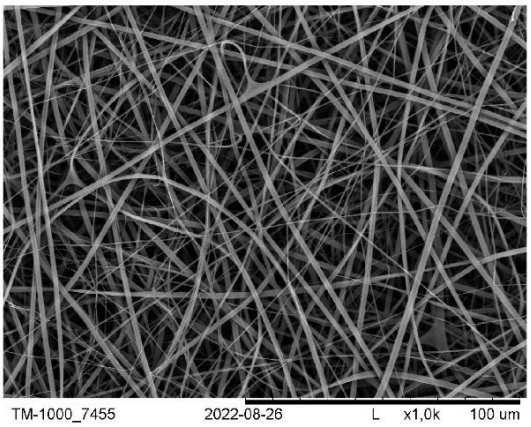

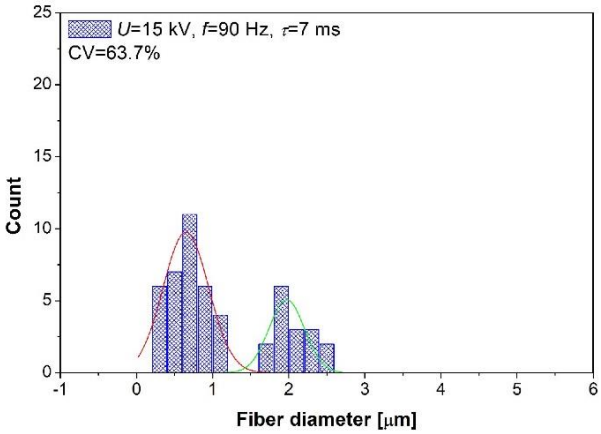

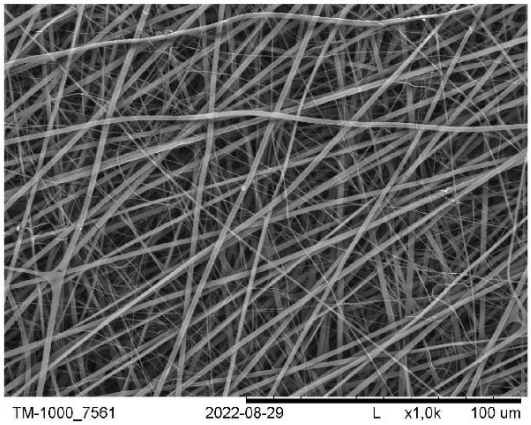

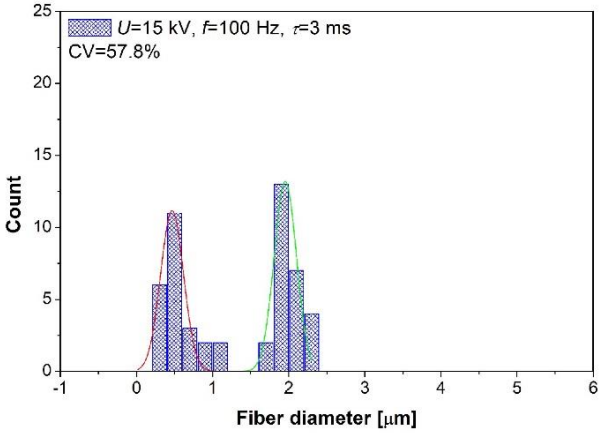

Figure 5: Morphology and distribution of fibre diameters in electrospun mats at electrical voltage U=15 kV and at different frequency of the pulses (f) and pulse duration (τ) values. Types of nonwovens obtained: monomodal (A), quasi-bimodal (B) and bimodal (C). Normal distribution (solid line on the graphs).

In all examined cases, mats with smooth fibres were produced and differences were only observed in the diameters of these fibres. When the system was operated at an electrical voltage of 8 kV and over the entire range of f (30-100 Hz) and τ (1-9 ms), mainly electrospun mats with a monomodal distribution of fibres diameter were obtained (Figure 4). The CV values estimated for a sample of each non-woven mat obtained under the specified conditions do not exceed 20% in most cases. In contrast, when the system was operated at 15 kV the application of different electrospinning process conditions (f =30-100 Hz, τ =1-9 ms) led to electrospun mats with both monomodal, quasi-bimodal and bimodal distribution of fibres diameter in the electrospun mats (Figure 5). The SEM images and histograms obtained confirm a clear tendency for a parallel fraction of much thinner fibres to form when pulse frequencies above 60 Hz are applied (quasi-bimodal and bimodal fibres form). In the case of nonwovens with a bimodal distribution of fibers diameter, two clear fractions of fibers with diameters in the range of 0.25-1.25 μm and above 1.25 μm can be identified. It has also been estimated that for a bimodal distribution of mean diameters, the CV values are high and in the range of 40-65%. Table 2 illustrates the dependence of the type of nonwoven obtained on the conditions under which the electrospinning process was carried out. We can see that the electrical parameters (f and τ) strongly affect the morphology of the nonwovens obtained. In general, we can expect to obtain

bi- and quasi-bimodal fibres at frequencies in the range 50-70 Hz, but only at high pulse durations. On the other hand, at f in the range 80-100 Hz and τ in the range 2-9 ms we obtain mainly bimodal fibres (Table 2). Hence, the conclusion is that a very large amount of charge delivered to the system results in the appearance of an additional fraction of fine fibres.

Table 2: Process conditions for obtaining monomodal, quasi-bimodal and bimodal electrospun mats at *U*=15 kV

15 kV		Pulse duration [ms]								
		1	2	3	4	5	6	7	8	9
Frequency of the pulses [Hz]	10									
	20									
	30									
	40									
	50									
	60									
	70									
	80									
	90									
	100									

no product monomodal quasi-bimodal bimodal

As mentioned earlier, in recent years, the preparation of nonwovens with bimodal fibre diameter distribution (both by needle-free electrospinning and by single- and multi-needle methods) has been of interest to many researchers. Recent reports speak of submicrofibrous membranes with bimodal distribution, developed by Quan et al. [16] which exhibited excellent breaking strength and elastic modulus. A little early, Zhao et al. [20] designed structured low-resistance fibre filters made of bimodal fibres and demonstrated that cleanable nanofibre membranes are able to rapidly transfer moisture and effectively capture harmful PM2.5 particles. In turn, Mei et al. [21] constructed fibre membranes with a bimodal structure using conventional single-needle electrospinning. Such nonwoven membranes showed high filtration efficiency, low pressure drop, and higher quality factors compared to monomodal nonwoven

membranes [21]. Bimodal structures have broad prospects not only for filtration materials and fibre scaffolds, but also for applications in biomedicine and other fields. Rad et al. [19] fabricated a porous PCl/zein/gum arabic nanofibre scaffold with a bimodal diameter distribution. Such scaffolds exhibited high hydrophilic properties, favourable porosity (approximately 80%) and adequate tensile strength which determines their high potential for application in skin tissue engineering. In another study by Soliman et al. [22] constructed multiscale three-dimensional scaffolds with controlled bimodal decomposition, which offers significant improvements over conventional monomodal scaffolds in terms of both mechanical and biological performance. Such a novel scaffold exhibited better stiffness and strength compared to conventional scaffolds, and also had a more open pore structure, which increased cell motility and survival.

Factorial analysis

As mentioned earlier, the main objective of the present work was to investigate the influence of the electrical parameters of the process, such as electrical voltage (U), frequency of the pulses (f) and pulse duration (τ), on the morphology of the resulting electrospun mats. The variants of the experiments along with the results obtained (average fiber diameter, D) are shown in Table 3.

Table 3: Experimental variants for a 2^3 factorial design including the average diameter of the obtained fibers (D). SD is the standard deviation.

No.	U [kV]	f [Hz]	τ [ms]	***D* [µm]**	±SD [µm]
1	8	30	1	**0.91**	0.31
2	8	30	9	**2.64**	0.44
3	8	100	1	**3.36**	0.88

4	8	100	9	**2.86**	0.66
5	15	30	1	**1.04**	0.40
6	15	30	9	**2.42**	0.30
7	15	100	1	**1.83**	0.46
8	15	100	9	**1.58**	0.66

The relationship between the parameters of the electrospinning process and the average diameter of the fibres formed can be expressed using equation 7:

$$D = a_0 + a_U \cdot U + a_f \cdot f + a_\tau \cdot \tau + a_{Uf} \cdot Uf + a_{U\tau} \cdot U\tau + a_{f\tau} \cdot f\tau + a_{Uf\tau} \cdot Uf\tau \quad (7)$$

where: $a_U - a_{Uf\tau}$ – the model coefficients , U, f, τ – the process factors (electrical voltage, frequency of the pulses, pulse duration), D – the response (average fiber diameter).

In order to determine the model coefficients, a design matrix was prepared assigning +1 values to the high levels of process factors and −1 values to low ones (Table 4).

Table 4: Design matrix of a 2^3 factorial design

No.	U [kV]	f [Hz]	τ [ms]
1	8 (−1)	30 (−1)	1 (−1)
2	8 (−1)	30 (−1)	9 (+1)
3	8 (−1)	100 (+1)	1 (−1)
4	8 (−1)	100 (+1)	9 (+1)
5	15 (+1)	30 (−1)	1 (−1)
6	15 (+1)	30 (−1)	9 (+1)
7	15 (+1)	100 (+1)	1 (−1)

8	15 (+1)	100 (+1)	9 (+1)

The model matrix X (Table 5) was then constructed by adding column *I* to the design matrix corresponding to the constant term a_0 in equation 7.

Table 5: Model matrix of a 2^3 factorial design

No.	I	U	f	τ	Uf	$U\tau$	$f\tau$	$Uf\tau$
1	+1	−1	−1	−1	+1	+1	+1	−1
2	+1	−1	−1	+1	+1	−1	−1	+1
3	+1	−1	+1	−1	−1	+1	−1	+1
4	+1	−1	+1	+1	−1	−1	+1	−1
5	+1	+1	−1	−1	−1	−1	+1	+1
6	+1	+1	−1	+1	−1	+1	−1	−1
7	+1	+1	+1	−1	+1	−1	−1	−1
8	+1	+1	+1	+1	+1	+1	+1	+1

The determined values of the $a_0 - a_{Uf\tau}$ parameters are shown in Table 6.

Table 6: The model coefficiens determining the impact of electrical voltage (U), frequency of the pulses (f) and pulse duration (τ) on the average fiber diameter (D)

a_0	a_U	a_f	a_τ	a_{Uf}	$a_{U\tau}$	$a_{f\tau}$	$a_{Uf\tau}$
2.08	**-0.363**	**0.328**	**0.295**	**-0.340**	**-0.013**	**-0.483**	**0.075**

After inserting the values obtained into equation 7, the model equation (eq. 8) describing the relationship between the electrical parameters and the mean diameter of the fibres was obtained.

$$D = 2.08 - 0.363U + 0.328f + 0.295\tau - 0.340Uf - 0.013U\tau - 0.483f\tau + 0.075Uf\tau \quad (8)$$

Based on the model coefficients obtained (Table 6), the electrical voltage (*U*), frequency of the pulses (*f*) and pulse duration (τ) were found to have comparable effects on the mean values of fibre diameters (*D*). Positive coefficients a_f and a_τ indicate that the variables *D*, *f*, τ are directly proportional and that the mean value of fibre diameter (*D*) increases with increasing *f* and τ. In contrast, the negative coefficient a_U confirms that the variables *D* and *U* are inversely proportional, with the mean value of the fibre diameter decreasing as U increases. Furthermore, of the other model coefficients collected in Table 6 (a_{Uf}, $a_{U\tau}$, $a_{f\tau}$, $a_{Uf\tau}$), only the variable *D* and the product of *U*, *f*, τ are also directly proportional, as confirmed by the positive coefficient $a_{Uf\tau}$. However, the change in fiber diameter (D) is most affected by the product of *f* and τ, as evidenced by the highest value of the coefficient $a_{f\tau}$ of 0.483.

Based on Eq. 8, 3D plots were generated (Figures 6, 8 and 10), which allow a comprehensive description of the interplay between the electrical parameters and the diameters of the fibres obtained. In addition, the diagrams drawn up are intended to help find the conditions under which fibres of the expected diameter and morphology can be obtained.

Figure 6 shows the effect of pulse duration (τ) and electrical voltage (*U*) on the diameter of the fibres produced (*D*) at minimum (30 Hz) and maximum (100 Hz) frequency (*f*).

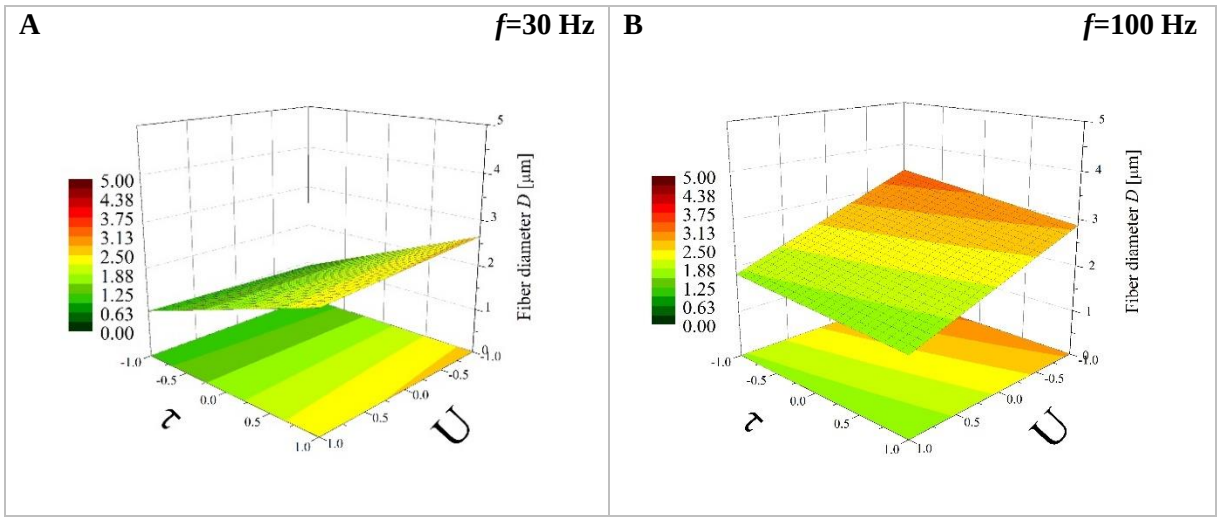

Figure 6: Response surface plots presenting the dependence of the diameter of the obtained fibers *(D)* on the pulse duration (τ) and the electrical voltage (U) for **(A)** minimum frequency of the pulses (*f*=-1, 30 Hz) and **(B)** maximum frequency of the pulses (*f*=1, 100 Hz).

For frequencies at low levels (30 Hz) (Figure 6A), the pulse duration (τ) affects the diameter of the fibres obtained to a much greater extent than the electrical voltage (*U*), and changing τ from low to high values (from 1 ms to 9 ms) increases *D* from approximately 0.75 µm to 1.75 µm. Furthermore, changing *U* from a low value to a high value (from 8 kV to 15 kV) causes only a small change in the thickness of the fibres obtained (from 1.75 to 2.0 µm). The situation is quite opposite for the maximum frequency (100 Hz) (Figure 6B). The electrical voltage then affects the diameters of the resulting fibers, and the *D* values change: in the case of 8 kV electrical operation, the average fibre diameters are above 2.0 µm, while in the case of 15 kV electrical operation, the *D* values are equal to approximately 1.25 µm. In contrast, the pulse duration (τ) in this case has no effect on the thickness of the fibres produced.

The results obtained from the 2^3 full factorial design correspond very well with those obtained experimentally (Figure 7). For *f* at low level (30 Hz) and τ=5-9 ms, the effect of electrical voltage (U) on *D* is negligible (Figure 7A). Differences in the thickness of the fibers produced at 8 and 15 kV are visible only for τ=2-4 ms. In the case of f at high level (100 Hz)

on the other hand, the fibres obtained at high electrical voltage (15 kV) are about half as thin as those obtained at lower electrical voltage (8kV) (Figure 7B).

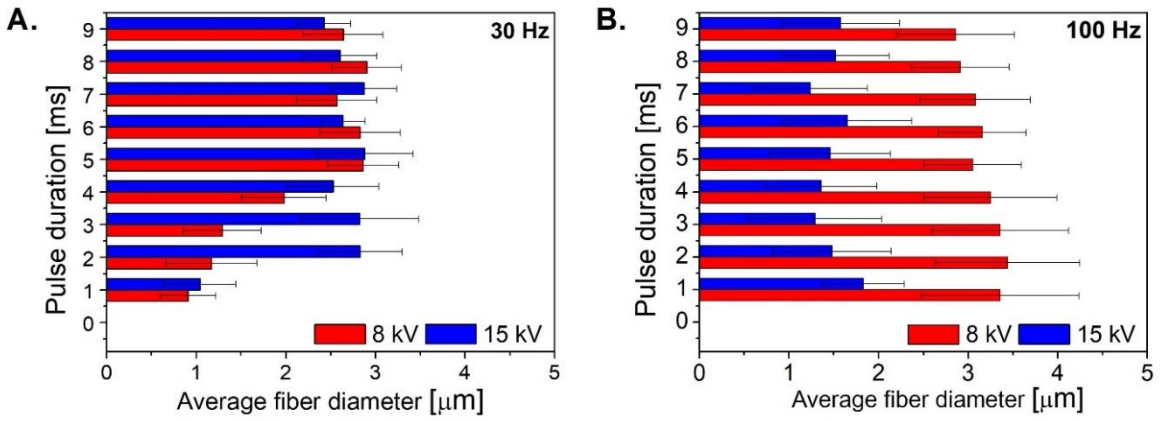

Figure 7: The effect of electrical voltage (*U*) on the average fiber diameters obtained by electrospinning depending on the frequency of the pulses: (A) 30 Hz, (B) 100 Hz used in the electrospinning process.

Figure 8 shows the effect of frequency (*f*) and pulse duration (*τ*) on the diameter of the fibres produced (*D*) at minimum (8 kV) and maximum (15 kV) electrical voltage (*U*).

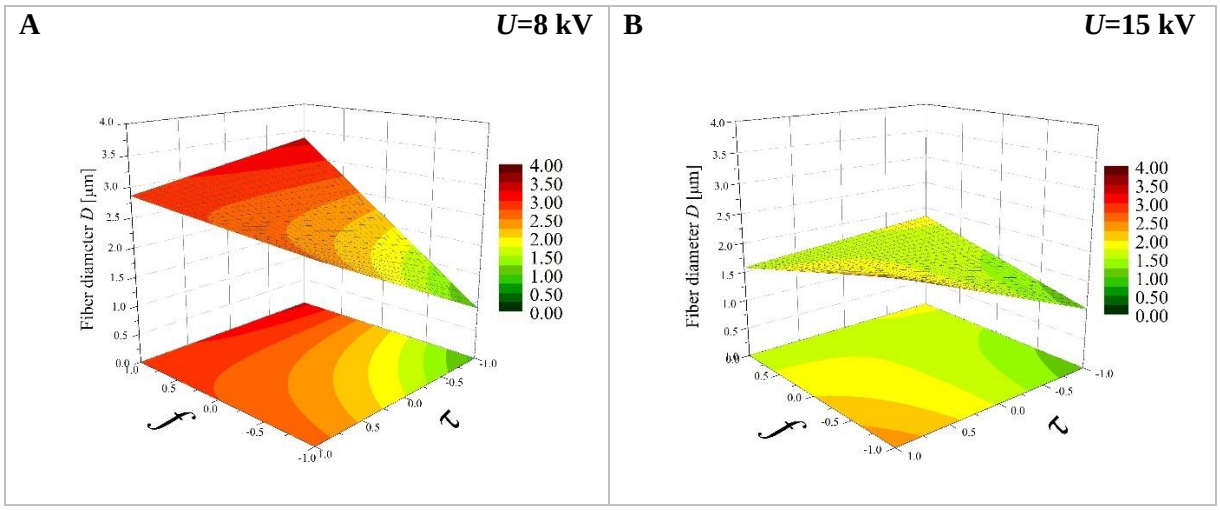

Figure 8: Response surface plots presenting the dependence of the diameter of the obtained fibers *(D)* on the frequency of the pulses (f) and the pulse duration (τ) for **(A)** minimum electrical voltage (*U*=-1, 8 kV) and **(B)** maximum electrical voltage (*U*=1, 15 kV).

For an electrical voltage (*U*) at a low level (8 kV) (Figure 8A), the pulse duration (τ) affects the fibre diameter much more than the frequency (*f*). A change in f (from 30 Hz to 100 Hz) causes little change in the value of *D* (2.5-2.72 µm). However, a change in τ (from 1 ms to 9 ms) causes the diameter to increase gradually from low values (about 1 µm) to high values (2.75 µm). This confirms that, by operating only on the pulse duration, fibres of the desired thickness can be easily obtained. Interestingly, for electrical voltage at high levels (15 kV), the fibre diameters decrease (from 2.25 to 1.5 µm) with increasing frequency (*f*) and increase (from 1 to 2 µm) with increasing pulse duration (Figure 8B). In this case, there is also a specific range of coefficients (light green area in Figure 8B) in which even small changes in their values do not result in changes in the value of the average fibre diameter.

Figure 9 shows the effect of frequency (*f*) and electrical voltage (*U*) on the diameter of the fibres produced (*D*) at minimum (1 ms) and maximum (9 ms) pulse duration (τ).

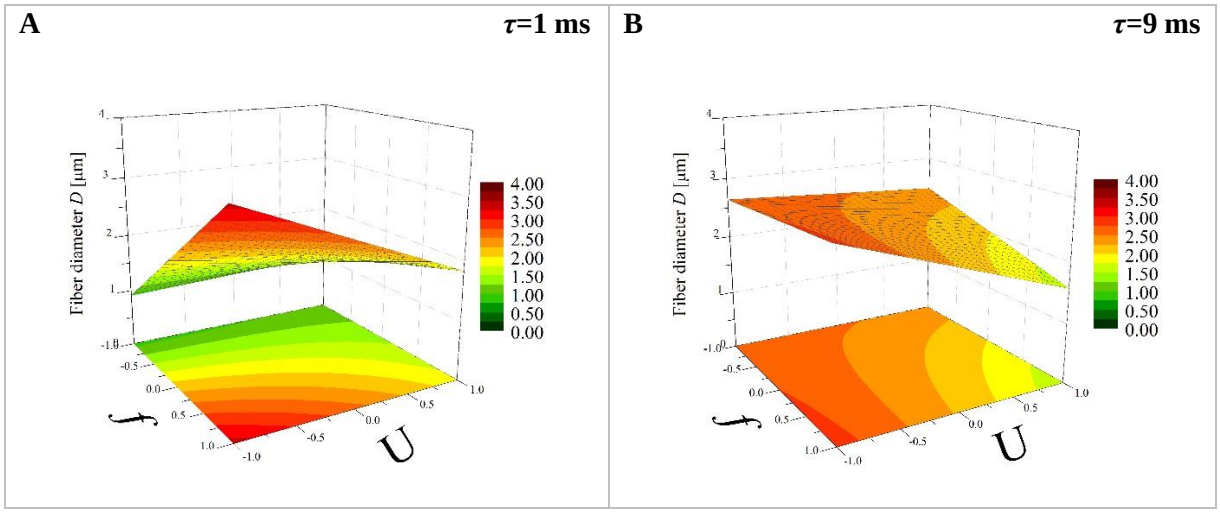

Figure 9: Response surface plots presenting the dependence of the diameter of the obtained fibers (D) on the frequency of the pulses (f) and the electrical voltage (U) for **(A)** minimum pulse duration (τ=-1, 1 ms) and **(B)** maximum pulse duration (τ=1, 9 ms).

For pulse durations (τ) at a low level (1 ms) (Figure 9A) the largest changes in diameter were observed. The increase in average fibre diameter (from 0.75 to even more than 3 µm) is directly proportional to the increasing value of the frequency in the process carried out. At the same

time, the relationship between the average fibre diameter and the electrical voltage is inversely proportional (the higher the voltage, the thinner the fibres obtained). In addition, it is important to highlight the fact that, with τ at a low level (1 ms), both electrical parameters (f and U) affect the size of the polymer fibre. Thus, valuable information from the factor analysis is that the greatest possibility of controlling the electrospinning process to obtain the desired product is observed at τ=1 ms. On the other hand, for τ at a high level (9 ms), the thickness of the fibre depends only on changes in the electrical voltage (U) (Figure 9B) but the range of changes in diameter is incomparably smaller than for τ=1 ms.

Similar effects were observed when analysing the results obtained experimentally (Figure 10). For pulse durations at a low level (1 ms), the electrical voltage has a large effect on the D of the fibres obtained. The application of U=15 kV leads to thicker fibres (with the exception of fibres obtained at f=100 Hz) (Figure 10A). On the other hand, for pulse durations at a high level (9 ms), the application of a high electrical voltage (15 kV) leads to thinner fibres than when a lower electrical voltage (8 kV) is applied (Figure 10B), especially for pulse frequencies above 60 Hz. At lower f (below 60 Hz), the average diameters of the fibres obtained at 8 kV and 15 kV are similar (Figure 10B).

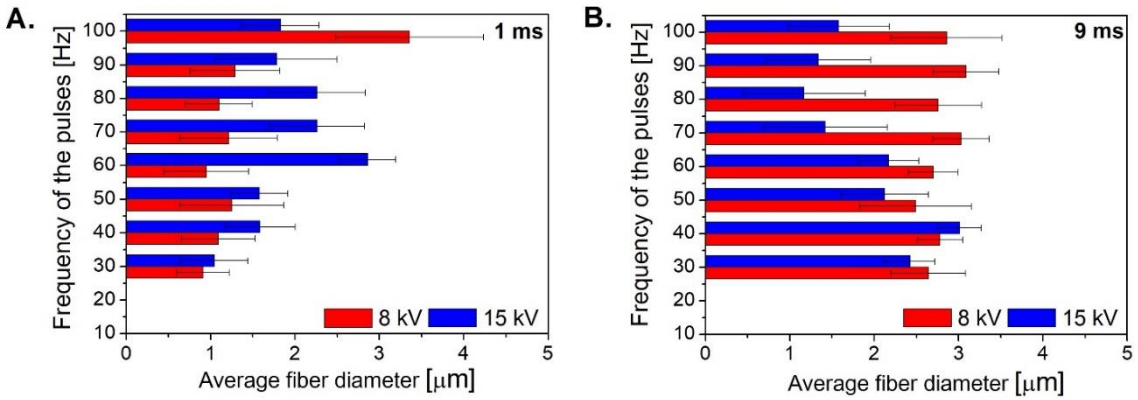

Figure 10: The effect of electrical voltage (U) on the average fiber diameters obtained by electrospinning depending on the pulse duration: (A) 1 ms, (B) 9 ms used in the process.

In this work, factor analysis was also applied to determine the effect of the electrical parameters of the process, in this case only the pulse frequency (f) and pulse duration (τ), on the standard deviation estimated for the average fibre diameters obtained from the electrospinning process. The experimental variants, together with the results obtained (standard deviation, SD) are shown in Table 7.

Table 7: Experimental variants for a 2^2 factorial design with the obtained mean standard deviation (SD)

No.	U [kV]	f [Hz]	τ [ms]	D [µm]	**±SD [µm]**
5	15	40	1	1.59	**0.41**
6	15	40	9	3.01	**0.26**
7	15	70	1	2.26	**0.57**
8	15	70	9	1.42	**0.74**

The effect of the electrospinning process parameters (in this case only f and τ) on the standard deviation (SD) for the mean fibre diameters can be expressed by equation 9:

$$SD = a_0 + a_f \cdot f + a_\tau \cdot \tau + a_{f\tau} \cdot f\tau \quad (9)$$

where: a_f – $a_{f\tau}$ – the model coefficients, f, τ – the process factors (frequency of the pulses, pulse duration), SD – the response (standard deviation).

To determine the model coefficients as above, a design matrix was prepared, assigning high levels of process factors a value of +1 and low levels a value of -1 (Table 8).

Table 8: Design matrix of a 2^2 factorial design

No.	f [Hz]	τ [ms]

1	40 (−1)	1 (−1)
2	40 (−1)	9 (+1)
3	70 (+1)	1 (−1)
4	70 (+1)	9 (+1)

The model matrix X (Table 9) was then constructed by adding column *I* to the design matrix corresponding to the constant term a_0 in equation 9.

Table 9: Model matrix of a 2^2 factorial design

No.	I	f	τ	$f\tau$
1	+1	−1	−1	+1
2	+1	−1	+1	−1
3	+1	+1	−1	−1
4	+1	+1	+1	+1

The determined values of the $a_0 - a_{f\tau}$ parameters are shown in Table 10.

Table 10: The model coefficiens determining the impact of frequency of the pulses (f) and pulse duration (τ) on the standard deviation (SD)

a_0	a_f	a_τ	$a_{f\tau}$
0.50	**0.16**	**0.01**	**0.08**

After inserting the values obtained into equation 9, the model equation (eq. 10) describing the relationship between the electrical parameters and the standard deviation.

$$\boldsymbol{SD = 0.50 + 0.16f + 0.01\tau + 0.08f\tau} \quad (10)$$

Based on the model coefficients obtained (Table 10), it was found that the standard deviation (*SD*) of the mean values of the fibre diameters obtained is most influenced by the frequency of the pulses (*f*). Of much lesser importance is the pulse duration (τ).

Conclusion

In this study, an attempt was made for the first time to determine how the electrical parameters of the pulsed electrospinning process: electrical voltage (*U*), frequency of the pulses (*f*) and pulse duration (τ), affect the morphology of the nonwovens manufactured. The results obtained and their detailed analysis allowed a general conclusion to be drawn: all the studied electrical parameters of the electrospinning process of 17% polyvinylpyrrolidone (PVP) solution strongly influence the average diameter (*D*) of the fibres obtained. It was found that the electrospinning process carried out at an electrical voltage of 8 kV leads to nonwovens with a monomodal fibre distribution. Under these conditions and using lower pulse durations (τ<5 ms), it was possible to obtain fibres with different diameters (from 1 to more than 3 μm), while using higher pulse durations (τ>5 ms) produced coarse fibres (*D*=approx. 3 μm). Furthermore, the electrospinning process carried out under an electrical voltage of 15 kV, with frequency of the pulses (*f*) in the range of 30-50 Hz and pulse durations (τ) above 2 ms, leads to fibres with average diameters of approx. 2.5-3 μm. In contrast, when *f*=80-100 Hz the average diameters of the fibres obtained are about 1.5 μm. In addition, the application of an electrical voltage of 15 kV and such high frequency of the pulses (80-100 Hz), we observe the coexistence of a fraction of finer and thicker fibres. According to the available literature, such nonwovens with a bimodal fibre distribution may have a number of interesting applications.

In the second part of the study, a 2^3 factorial design was used to determine how the selected electrical parameters of the electrospinning process affect the structure of the obtained electrospun mats. Among other things, it was shown that, by appropriately selecting the

electrical process parameters (U, f, τ), it is possible to control the thickness of the fibres obtained and, consequently, to obtain nonwovens with the desired morphology. Furthermore, the results obtained experimentally corresponded very well with the relationships established by means of a 2^3 factorial design. Thus, it was confirmed that it is not necessary to carry out multiple tests in order to find a nonwoven with a suitable morphology. Factor analysis proves itself as a useful tool for the design of electrospinning processes.

Funding

The research was funded by Nalecz Institute of Biocybernetics and Biomedical Engineering Polish Academy of Sciences.

References

(1) Bhattarai, R. S.; Bachu, R. D.; Boddu, S. H. S.; Bhaduri, S. *Pharmaceutics 2019, Vol. 11, Page 5* **2018**, *11*, 5. doi:10.3390/PHARMACEUTICS11010005

(2) Rahmati, M.; Mills, D. K.; Urbanska, A. M.; Saeb, M. R.; Venugopal, J. R.; Ramakrishna, S.; Mozafari, M. *Prog Mater Sci* **2021**, *117*, 100721. doi:10.1016/J.PMATSCI.2020.100721

(3) Xue, J.; Wu, T.; Dai, Y.; Xia, Y. *Chem Rev* **2019**, *119*, 5298. doi:10.1021/ACS.CHEMREV.8B00593

(4) Wang, F.; Hu, S.; Jia, Q.; Zhang, L. *J Nanomater* **2020**, *2020*. doi:10.1155/2020/8719859

(5) Medeiros, G. B.; Lima, F. de A.; de Almeida, D. S.; Guerra, V. G.; Aguiar, M. L. *Membranes 2022, Vol. 12, Page 861* **2022**, *12*, 861. doi:10.3390/MEMBRANES12090861

(6) Rashid, T. U.; Gorga, R. E.; Krause, W. E. *Adv Eng Mater* **2021**, *23*, 2100153. doi:10.1002/ADEM.202100153

(7) Li, Y.; Zhu, J.; Cheng, H.; Li, G.; Cho, H.; Jiang, M.; Gao, Q.; Zhang, X. *Adv Mater Technol* **2021**, *6*. doi:10.1002/ADMT.202100410

(8) Shi, S.; Si, Y.; Han, Y.; Wu, T.; Iqbal, M. I.; Fei, B.; Li, R. K. Y.; Hu, J.; Qu, J. **2022**. doi:10.1002/adma.202107938

(9) Anaya Mancipe, J. M.; Boldrini Pereira, L. C.; de Miranda Borchio, P. G.; Dias, M. L.; da Silva Moreira Thiré, R. M. *J Biomed Mater Res B Appl Biomater* **2023**, *111*, 366–381. doi:10.1002/JBM.B.35156

(10) Huang, C.; Dong, J.; Zhang, Y.; Chai, S.; Wang, X.; Kang, S.; Yu, D.; Wang, P.; Jiang, Q. *Mater Des* **2021**, *212*, 110240. doi:10.1016/J.MATDES.2021.110240

(11) Mahmud, M. M.; Zaman, S.; Perveen, A.; Jahan, R. A.; Islam, M. F.; Arafat, M. T. *J Drug Deliv Sci Technol* **2020**, *55*, 101386. doi:10.1016/J.JDDST.2019.101386

(12) Li, K.; Wang, Y.; Xie, G.; Kang, J.; He, H.; Wang, K.; Liu, Y. *J Appl Polym Sci* **2018**, *135*. doi:10.1002/APP.46130

(13) Xie, G.; Wang, Y.; Han, X.; Gong, Y.; Wang, J.; Zhang, J.; Deng, D.; Liu, Y. *Ind Eng Chem Res* **2016**, *55*, 7116–7123. doi:10.1021/ACS.IECR.6B00958/SUPPL_FILE/IE6B00958_SI_001.PDF

(14) Mirek, A.; Grzeczkowicz, M.; Belaid, H.; Bartkowiak, A.; Barranger, F.; Abid, M.; Wasyłeczko, M.; Pogorielov, M.; Bechelany, M.; Lewi´nskalewi´nska, D. **2023**. doi:10.1016/j.bioadv.2023.213330

(15) Mirek, A.; Korycka, P.; Grzeczkowicz, M.; Lewi, D. **2019**. doi:10.1016/j.matdes.2019.108106

(16) Quan, Z.; Wang, Y.; Zu, Y.; Qin, X.; Yu, J. *Eur Polym J* **2021**, *159*. doi:10.1016/J.EURPOLYMJ.2021.110707

(17) Tomadakis, M.; Fuselier, K.; Almeer, F.; Ferguson, A.; Cowdrick, V. *Chem Eng Sci* **2020**, *212*, 115298. doi:10.1016/J.CES.2019.115298

(18) Mirek, A.; Korycka, P.; Grzeczkowicz, M.; Lewińska, D. *Mater Des* **2019**, *183*. doi:10.1016/J.MATDES.2019.108106

(19) Pedram Rad, Z.; Mokhtari, J.; Abbasi, M. *Materials Science and Engineering: C* **2018**, *93*, 356–366. doi:10.1016/J.MSEC.2018.08.010

(20) Zhao, X.; Li, Y.; Hua, T.; Jiang, P.; Yin, X.; Yu, J.; Ding, B. *Small* **2017**, *13*, 1603306. doi:10.1002/SMLL.201603306

(21) Mei, Y.; Wang, Z.; Li, X. *J Appl Polym Sci* **2013**, *128*, 1089–1094. doi:10.1002/APP.38296

(22) Soliman, S.; Pagliari, S.; Rinaldi, A.; Forte, G.; Fiaccavento, R.; Pagliari, F.; Franzese, O.; Minieri, M.; Di Nardo, P.; Licoccia, S.; Traversa, E. *Acta Biomater* **2010**, *6*, 1227–1237. doi:10.1016/J.ACTBIO.2009.10.051

(23) Korycka, P.; Mirek, A.; Kramek-Romanowska, K.; Grzeczkowicz, M.; Lewińska, D. *Beilstein J. Nanotechnol* **2018**, *9*, 2466–2478. doi:10.3762/bjnano.9.231

(24) Can-Herrera, L. A.; Oliva, A. I.; Dzul-Cervantes, M. A. A.; Pacheco-Salazar, O. F.; Cervantes-Uc, J. M. *Polymers 2021, Vol. 13, Page 662* **2021**, *13*, 662. doi:10.3390/POLYM13040662

(25) Sivan, M.; Madheswaran, D.; Valtera, J.; Kostakova, E. K.; Lukas, D. *Mater Des* **2022**, *213*, 110308. doi:10.1016/J.MATDES.2021.110308

(26) Bingol, D.; Tekin, N.; Alkan, M. *Appl Clay Sci* **2010**, *50*, 315–321. doi:10.1016/J.CLAY.2010.08.015

(27) Tarley, C. R. T.; Silveira, G.; dos Santos, W. N. L.; Matos, G. D.; da Silva, E. G. P.; Bezerra, M. A.; Miró, M.; Ferreira, S. L. C. *Microchemical Journal* **2009**, *92*, 58–67. doi:10.1016/J.MICROC.2009.02.002

(28) Ramlow, H.; Marangoni, C.; Motz, G.; Machado, R. A. F. *Chemical Engineering Journal Advances* **2022**, *9*, 100220. doi:10.1016/J.CEJA.2021.100220

(29) Enis, I. Y.; Sezgin, H.; Sadikoglu, T. G. *Journal of Industrial Textiles* **2018**, *47*, 1378–1391. doi:10.1177/1528083717690614

(30) Nawinda, C.; Sirikarn, P.; Chutima, L.; Limmatvapirat, S. *Key Eng Mater* **2017**, *757 KEM*, 120–124. doi:10.4028/WWW.SCIENTIFIC.NET/KEM.757.120

(31) Tong, H. W.; Wang, M. *J Appl Polym Sci* **2011**, *120*, 1694–1706. doi:10.1002/APP.33302

(32) Mirek, A.; Grzeczkowicz, M.; Lamboux, C.; Sayegh, S.; Bechelany, M.; Lewińska, D. *Colloids Surf A Physicochem Eng Asp* **2022**, *648*, 129246. doi:10.1016/J.COLSURFA.2022.129246

(33) Lewińska, D.; Rosiński, S.; Weryński, A. *Artif Cells Blood Substit Immobil Biotechnol* **2004**, *32*, 41–53. doi:10.1081/BIO-120028667